1 **Revision 1**

2 **Extraterrestrial, shock-formed, cage-like nanostructured carbonaceous materials**

3 Péter Németh[1,2] and Laurence A.J. Garvie[2,3]

4 [1]Institute of Materials and Environmental Chemistry, Research Center for Natural Sciences,

5 Hungarian Academy of Sciences, H-1117 Budapest, Magyar Tudósok Körútja 2, Hungary.

6 [2]School of Earth and Space Exploration, [3]Center for Meteorite Studies, Arizona State

7 University, Tempe, Arizona 85287-6004, USA.

8 *Correspondence to: nemeth.peter@ttk.mta.hu*

9

10

ABSTRACT

11

12   Shock caused by impacts can convert carbonaceous material to diamond. During this transition, new

13   materials can form that depend on the structure of the starting carbonaceous materials and the shock

14   conditions. Here we report the discovery of cage-like nanostructured carbonaceous materials, including

15   carbon nano-onions and bucky-diamonds, formed through extraterrestrial impacts in the Gujba (CB_a)

16   meteorite. The nano-onions are fullerene-type materials and range from 5 to 20 nm; the majority shows

17   a graphitic core-shell structure, and some are characterized by fully curved, onion-like graphitic shells.

18   The core is either filled with carbonaceous material or empty. We show the first, natural, 4-nm-sized

19   bucky-diamond, which is a type of carbon nano-onion consisting of multilayer graphitic shells

20   surrounding a diamond core. We propose that the nano-onions formed during shock metamorphism,

21   either the shock or the release wave, of the pre-existing primitive carbonaceous material that included

22   nanodiamonds, poorly-ordered graphitic material, and amorphous carbonaceous nanospheres. Bucky-

23   diamonds could have formed either through the high-pressure transformation of nano-onions, or as an

24   intermediate material in the high-temperature transformation of nanodiamond to nano-onion. Impact

25   processing of planetary materials was and is a common process in our Solar System, and by extension,

26   throughout extrasolar planetary bodies. Together with our previous discovery of interstratified graphite-

27   diamond in Gujba, our new findings extend the range of nano-structured carbonaceous materials

28   formed in nature. Shock-formed nano-onions and bucky-diamonds are fullerene-type structures, and as

29   such could contribute to the astronomical 217.5 nm absorption feature.

30

31

INTRODUCTION

32

33   Shock metamorphism resulting from hypervelocity impacts is a fundamental process in our Solar

34   System (Sharp and DeCarli 2006). It plays a major role in planetary evolution and is evidenced by

35   shock-induced modifications in minerals and formation of high-pressure and high-temperature phases

36   (e.g., Chen et al. 1996; El Goresy et al. 2008). The nature of these modifications strongly depends on

37   the material and the shock conditions (Sharp and DeCarli 2006). Since shock metamorphism is a rapid

38   event, during which pressure equilibration can be completed within nano- or microseconds after

39   impact, novel materials may form and be quenched (Chao et al. 1962; Chen et al. 1996; Sharp et al.

40   1997, 1999). There has been considerable interest in shock compression of carbonaceous material, of

41   which the formation of diamond from graphitic material has been widely described (e.g., DeCarli and

42   Jamieson 1961; Erskine and Nellis 1991; Yamada and Tanabe 2002; LeGuillou et al. 2010). In addition

43   to diamond, a range of sp^2- and sp^3-bonded structures have been reported including defective and

44   stacking disordered diamond (Németh et al. 2014; Németh et al. 2015; Ohfuji et al. 2015; Murri et al.

45   2019), interstratified graphite-diamond (Garvie et al. 2014), amorphous- (Kis et al. 2016), and onion-

46   like carbons (Shumilova et al. 2014).

47   Carbonaceous chondrite meteorites contain a wide range of nano-structured materials encompassing

48   sp^3-bonded structures, dominated by nanodiamonds, and sp^2-bonded materials. Nanodiamonds are

49   present in the matrix of all unmetamorphosed carbonaceous chondrites, with matrix-normalized values

50   of ca. 700 to 1500 ppm (Huss and Lewis, 1995). Their small sizes, typically ~2 nm, and high

51   abundances, imply large numbers, on the order of 3×10^{17} nanodiamonds, per gram of matrix. The total

52   C content of unmetamorphosed carbonaceous chondrites varies from ~ 5 wt% in the CIs (Orgueil 4.88

53   wt%) to ~2 wt% for the CM2 (e.g., Murchison, 2.25 wt%) chondrites (Pearson et al. 2006). Much of

54   this C occurs as sp^2-bonded carbonaceous material, also called macromolecular carbon (Garvie and

55   Buseck, 2006). In HRTEM images, this material presents itself as poorly-ordered "graphitic material"

56   that typically has a crumpled tissue-like texture, with poorly ordered, small, irregularly-shaped regions

57   having fringes with 0.34–0.38 nm spacings and locally 0.21 nm cross-fringes. Also present are solid or

58   hollow carbon nanospheres: HRTEM images of these nanospheres are typically devoid of fringes

59   revealing their amorphous character (Garvie and Buseck, 2004; 2006). Well-crystallized graphitic

60   material is also present in the CC meteorites, but is less common.

61   Here we report the discovery of cage-like nanostructured carbonaceous materials, including carbon

62   nano-onions and bucky-diamonds from the Gujba (CB$_a$) meteorite. Carbon nano-onions are fullerene-

63   like structures consisting of spherical carbon shells (Ugarte 1992), whereas bucky-diamonds are

64   nanoparticles containing a nanodiamond covered by fullerene-like shells (Raty et al. 2003). Carbon

65   nano-onions are well-known from syntheses (Ugarte 1992; Kuznetsov et al. 1994a, b; Qin and Iijima

66   1996; Sano et al. 2001; Xiao et al. 2014), and although onion-like structures have previously been

67   described from the Murchison (Bernatowitz et al. 1996) and the martian meteorite Allan Hills 84001

68   (Steele et al. 2012) as well as from Popigai impact materials (Shumilova et al. 2014), those resembling

69   large multilayered fullerenes (Ugarte 1992; Xiao et al. 2014) have not been reported from natural

70   materials. Although, Smith and Buseck (1981) showed a nano-onion from Allende meteorite, the

71   authors argued that it might have been an artifact of the sample preparation. Our report is also the first

72   description of natural bucky-diamonds. We studied these nanocarbons with a view of shedding light on

73   their possible formation conditions and draw attention to their characteristic absorption feature at the

74   wavelength of 217.5 nm, which matches that of interstellar dust (Stecher 1965; Wright 1988;

75   Chhowalla et al. 2003; Bradley et al. 2005).

76

77   *Gujba meteorite*

78   Gujba belongs to a group of metal-rich meteorites called CB chondrites, and currently comprises 21

79   meteorites. Gujba belongs to the CB$_a$ subgroup and is characterized by ~60 vol% metal and cm-sized

80   chondrules separated by a sparse, often dark-colored, matrix (Weisberg and Kimura 2010). While the

81   origin of the CB chondrules has generated significant debate, it is generally accepted that they (and

82   similarly CH and CH/CB chondrites) are the end result of a combination of events that was initiated by

83   the glancing blow impact of two planetesimals (Asphaug et al. 2011), condensation of materials

84   including the metal spheres in the dense impact-formed metal-rich gas, followed by reaccretion on the

85   impacted parent body (Morris et al., 2015). Such a scenario was explored in detail for the Isheyevo

86   (CH/CB$_b$) meteorite (Morris et al. 2015; Garvie et al. 2017). Chondrules within the CB meteorites

87   Gujba are dated at 4562 Myr (Krot et al. 2005), which is ∼5.5 Myr after the formation of the calcium-

88   aluminum-rich inclusions (CAIs) of 4568.2 Myr (Bouvier and Wadhwa 2010) and 4567.3 Myr

89   (Connelly et al., 2017). However, the CB parent body also underwent a later major impact at ∼4200

90   Myr (Marty et al. 2010); evidence for this impact is a suite of high-pressure minerals (Garvie et al.

91   2011; Garvie et al, 2014; Weisberg and Kimura 2010; Weisberg et al. 2006).

92

93   **EXPERIMENTAL METHODS**

94   Transmission electron microscopy (TEM) samples were prepared from the carbonaceous residue

95   obtained from fragments of the Gujba meteorite interstitial to the metal following the protocol

96   described by Garvie et al. (2014). High-resolution TEM (HRTEM) images were acquired with a Tecnai

97   F20 (200 kV; Schottky field-emission gun, side-entry, double-tilt stage; point resolution = 0.24 nm), a

98   Topcon 002B (200 keV, LaB$_6$ filament, side entry, C_s = 0.4 mm, point resolution = 0.19 nm), and a

99   JEOL JEM 4000EX (400 kV; LaB$_6$ filament, top-entry, double-tilt stage; C_s = 1 mm; point resolution =

100   0.17 nm) electron microscope. Fast Fourier transforms (FFTs) obtained from the HRTEM images were

101   calculated using Gatan Digital Micrograph 3.6.1 software. Background-filtered images were calculated

102   by applying a mask filter on graphite and diamond reflections using the same software.

103

104   **RESULTS AND DISCUSSION**

105   HRTEM images of the Gujba acid residue reveal the structural diversity of carbonaceous particles

106   including amorphous to poorly graphitized carbon, ordered graphitic material, interstratified graphite-

107   diamond (Garvie et al. 2014), nanodiamonds, and cage-like nanostructured carbonaceous grains. The

108   nanodiamonds are small (2-3-nm) and typically aggregated (Fig. 1a), consistent with those found in un-

109   shocked carbonaceous chondrites (Garvie 2006; Daulton et al. 1996). Carbonaceous objects with

110   rounded morphology occur in the residue. In particular, compact (Fig. 1b) and hollow nanospheres

111   (Fig. 1c) occur, and they are similar in shape, size, and structure to those reported from a range of

112   carbonaceous chondrites (Nakamura-Messenger et al. 2006; Garvie 2005; Garvie and Buseck 2006).

113   Their size ranges between 20- and 200-nm, and according to Garvie (2006) their HRTEM and EELS

114   data are consistent with an essentially amorphous material, although regions with poorly ordered

115   graphite can also be detected (Figs. 1b and 1c). They are dominated by carbon and contain minor

116   amounts of sulfur, nitrogen and oxygen (Garvie 2006) and possibly some hydrogen (Naraoka et al.

117   2004).

118   In addition to the afore-mentioned carbonaceous materials, we discovered nano-sized cage-like

119   nanostructured carbonaceous materials in the residue. These cage-like materials are prominent in the

120   HRTEM images, and are visible as individual particles composed of concentric graphitic shells.

121   Approximately 40 nano-onions were imaged and their sizes ranged from 5 and 20 nm (Fig. 2). They

122   have similar morphologies to synthetic nano-onions (Ugarte 1992; Xiao et al. 2014). Many of the nano-

123   onions are attached to or spatially associated with grains of interstratified graphite-diamond.

124   The nano-onions are characterized by concentric graphitic shells with 0.34-0.35 nm spacing around

125   a hollow or filled core. The continuity of these spacings around the core is consistent with a nested

126   shell-like with structure of graphitic shells. Most nano-onions showed between 5 and 10 graphitic

127   shells, and the largest contained 30 shells (Fig. 2a). The nano-onions are either hollow (Figs. 2a, 2b, 2c,

128   and 2d) or filled (Figs. 2e and 2f). According to literature reports (Terrones and Terrones, 1997), the

129   cores could be crystalline or amorphous, although in our sample we only identified crystalline core

130   materials. Some HRTEM images show cores with 0.21-nm spacings, consistent with both graphite and

131   diamond (Figs. 2e and 2f). The d-spacing of graphite {100} is 0.212 nm and that of diamond {111} is

132   0.206 nm. The experimental error of the d-value measurements from HRTEM images is ~ 2-5 %,

133   therefore, distinguishing between graphite and diamond based on one set of 0.21-nm fringes alone is

134   not possible. However, graphite and diamond can be identified by the 60° and 71° 0.21-nm cross-

135   fringes, respectively.

136   One nano-onion was found fortuitously oriented so that its central part showed fringes consistent

137   with graphite projected along <001> (Fig. 3). Since an HRTEM image is a 2D projection of a 3D

138   object, this graphite could be in the core of a nano-onion or part of its shell occurring on the top or the

139   bottom of the onion. If it occurred inside the onion, it would be a new type, the first graphite-filled

140   nano-onion.

141   A single caged nano-onion was discovered that shows a distinct diamond core (Fig. 4) containing

142   {111} diamond reflections in <110> projection. Visible are the 0.206-nm spacings of the {111} planes

143   with 71° cross fringes. This caged-nanostructure is a special type of nano-onion referred as bucky-

144   diamond (Barnard et al. 2003; Raty et al. 2003).

145   The carbonaceous materials in Gujba reflect the diversity of structures acquired and formed under a

146   range of environments including, unmodified materials primarily from the impactor, formation and

147   modification in the impact plume during cooling and condensation, reaccretion on the planetesimal,

148   and finally modification by post-accretion shock events. The similarities in mineral and O isotopic

149   compositions of the CB ($\Delta^{17}O \sim -2‰$) and CR ($\Delta^{17}O = -4‰$ to 0‰) chondrites suggest a common

150   nebular reservoir (Krot et al. 2006). Hence the precursor carbonaceous materials were likely similar to

151   those found in primitive, unmetamorphosed carbonaceous chondrites, such as CM2 and CR2

152   chondrites. We propose that both nanodiamonds (Fig. 1a) and the poorly-ordered, amorphous

153   nanospheres (Figs. 1b and 1c) of the Gujba meteorite are the precursor materials for the cage-like

154   nanostructured carbonaceous materials (Figs. 2, 3, and 4).

155   The close association of many of the nano-onions with grains of interstratified graphite-diamond is

156   consistent with contemporaneous formation of both during the same shock event. The materials could

157 have formed during the initial shock wave or during the release wave following the initial shock

158 compression, when the local structures were placed under tension. The Gujba peak shock conditions

159 are estimated to be 2273 K and 19 GPa based on a suite of minerals formed at high pressure and

160 temperature including majorite garnet, wadsleyite, coesite, and stishovite (Weisberg and Kimura 2004;

161 Weisberg et al. 2006, Garvie et al. 2014). However, the complex and heterogeneous structure of the

162 Gujba meteorite would have produced significant mm-scale pressure and temperature variations.

163 Structurally, the Gujba meteorite is characterized by millimeter-sized metal spheres separated by

164 silicate clasts and dark interstitial matrix (Rubin et al. 2003). The metal has higher shock impedance

165 than the surrounding silicate-rich material, which would have produced significant differences in the

166 shock conditions of the metal globules and surrounding material. Different shock velocities between

167 metal and silicates could result in irregular shock front propagating through Gujba. In addition, the

168 shock fronts can be refracted at the metal/silicate boundary producing localized, millimeter- to

169 micrometer-scale, pressure spikes of nanoseconds duration in the low-impedance material. The peak

170 pressures and temperature associated can vary by over an order of magnitude over short spatial

171 distances, with pressure equilibration within a microsecond and temperature equilibration within

172 seconds (Sharp and DeCarli, 2006). These small spatial-scale shock heterogeneities explain the

173 observed association of unshocked carbonaceous materials, such as poorly ordered graphite,

174 amorphous nanospheres and nanodiamonds, together with the shock-formed cage-like nanostructured

175 carbonaceous materials.

176   Carbon nano-onions were first produced by intense electron irradiation of carbon soot in a

177 TEM (Ugarte 1992). They were later found in detonation soot (Kuznetsov et al. 1994b) and were

178 synthesized via a variety of methods including arc discharge of graphite in liquids (Sano et al. 2001)

179 and combustion of naphthalene (Choucair and Stride 2012). Nano-onions can be prepared from

180 nanodiamonds through heat treatment (Kuznetsov et al. 1994a), electron irradiation (Qin, L-C. and

181 Iijima 1996), and at high pressures (Blank et al. 2007, 2018). Nano-onions can also be formed directly

182   from graphite in a diamond anvil (>20 GPa) under shear deformation at room temperature (Blank et al.,

183   2007), with nano-onion size increasing with increase of pressure and shear values. At higher pressures,

184   >55GPa, diamond also transforms to onion-like structure (Blank et al. 2018). According to Blank et al.

185   (2009), the formation of onions appears to be a "dead-end branch of high-pressure graphite

186   transformations". However, Xiao et al. (2014) showed that during energetic irradiation, it is possible to

187   convert nanodiamonds to nano-onions, which upon further irradiation can convert back to nano-onions.

188   The reversible transition occurs via the bucky-diamond intermediary phase.

189   The structural and textural complexity of the starting carbonaceous material in the Gujba meteorite,

190   together with the wide range of P and T conditions present during the shock, suggests several

191   mechanisms and starting materials in their formation. Firstly, the nano-onions and bucky-diamonds

192   may have formed through the shock processing of the pre-existing nanodiamonds. The small sizes of

193   some of the cage-like onions are consistent with their formation from a nanodiamonds precursor (e.g.,

194   Figs. 2d, 2e, 2f, 3, and 4). It is possible that some of the larger, i.e., 10 to 20 nm nano-onions (Figs. 2a,

195   2b, and 2c) formed directly from the high-pressure transformation of the compact nanospheres.

196   Alternatively, the close association of some nano-onions with the interstratified diamond-graphite

197   particles suggests a common precursor material for both. The interstratified diamond-graphite

198   represents the incomplete formation of diamond from graphitic material and forms short stubby grains

199   to a few tens of nanometer in length (Garvie et al. 2014). These stubby grains likely formed from the

200   shock-transformation of the poorly ordered graphitic material that is common in carbonaceous

201   chondrites of low petrologic grade. This poorly ordered carbon forms ribbons with short flat regions

202   and curved morphologies. We suggest that the interstratified diamond-graphite formed within the flat

203   areas of the ribbons and the nano-onions along the curved areas.

204   <center>**IMPLICATIONS**</center>

205   *Nano-onions, bucky-diamonds and the interstellar 217.5 nm absorption feature*

206   A prominent feature of the interstellar dust ultraviolet absorption spectrum is a broad bump at 217.5

207   nm (Stecher 1965, Wright 1988; Bradley et al. 2005). Understanding the origin of this feature is still a

208   major issue in astronomy. The feature is peculiar as the central wavelength is spatially invariant, but its

209   bandwidth varies from one line to another, suggesting multiple carriers or a single carrier with variable

210   properties. Bradley et al. (2005) associated the astronomical feature with organic carbon and

211   amorphous silicates found in interplanetary dust particles, based on the spectral similarities of these

212   materials. According to literature reports, the feature could match that of carbon nano-onions (Wright

213   1988; Chhowalla et al. 2003) and presumably bucky-diamonds since they also contain fullerene-type

214   structure. However, extraterrestrial onion-like objects have so far only been reported from the martian

215   meteorite Allan Hills 84001 (Steele et al. 2012). This report shows the finding of nano-onions and

216   bucky-diamonds from Gujba meteorite and proposes that fullerene-type materials could form from the

217   primitive carbonaceous material during impact, a fundamental geological process in the universe. Thus,

218   we suggest that carbonaceous onion-type objects could be common in the Solar System and a

219   component of the 217.5 nm astronomical feature.

226

227

228 **References cited**

229 Asphaug, E., Jutzi, M., and Movshovitz, N. (2011) Chondrule formation during planetesimal accretion.

230   Earth Planetary Science Letters, 308, 369–379.

231 Barnard, A.S., Russo, S.P., and Snook, I.K. (2003) Coexistence of bucky diamond with nanodiamond

232   and fullerene carbon phases. Physical Review B, 68, 073406 (1-4).

233 Bernatowicz, T.J., Cowsik R., Gibbons, P.C., Lodders, K., Fegley, B., Amari, S., and Lewis, R.S.

234   (1996) Constraints on Stellar Grain Formation from Presolar Graphite in the Murchison

235   Meteorite. The Astrophysical Journal, 472, 760-782.

236 Bouvier, A., and Wadhwa, M. (2010} The age of the Solar System redefined by the oldest Pb-Pb age of

237   a meteoritic inclusion. Nature Geosciences, 3, 637–641.

238 Blank, V.D., Denisov, V.N., Kirichenko, A.N., Kulnitskiy, B.A., Martushov, S.Y., Mavrin, B.N., and

239   Perezhogin, I.A. (2007) High pressure transformation of single-crystal graphite to form molecular

240   carbon–onions. Nanotechnology, 18, 345601.

241 Blank, V.D., Churkin, V.D., Kulnitsky, B.A., Perezhogin, I.A.., Kirichenko, A.N., Erohin, S.V.,

242   Sorokin, P.B., and Popov, M.Y. (2018) Pressure-Induced Transformation of Graphite and

243   Diamond to Onions. Crystals, 8(2), 68.

244 Bradley, J., Dai, Z.R., Erni R., Browning, N., Graham, G., Weber P., Smith, J., Hutcheon, I., Ishii, H.,

245   Bajt, S., Floss, C., Stadermann, F., and Standford, S. (2005) An Astronomical 2175 Å Feature in

246   Interplanetary Dust Particles. Science, 307, 244-247.

247 Chao, E.T.C., Fahey, J.J., Littler, J., and Milton, D.J. (1962) Stishovite, SiO_2, a very high pressure new

248   mineral from Meteor Crater, Arizona. Journal of Geophysical Research, 67, 419-421.

249 Chen, M., Sharp, T.G., El Goresy, A., Wopenka, B., and Xie, X. (1996) The Majorite-Pyrope +

250   Magnesiowüstite Assemblage: Constraints on the History of Shock Veins in Chondrites. Science,

251   271, 1570-1573.

252   Chhowalla, M., Wang, H., Sano, N., Teo, K.B.K., Lee, S.B., and Amaratunga, G.A.J. (2003) Carbon

253   Onions: Carriers of the 217.5 nm Interstellar Absorption Feature. Physical Review Letters, 90,

254   155504.

255   Choucair, M., and Stride, J.A. (2012) The gram-scale synthesis of carbon onions. Carbon, 50, 1109–

256   1115.

257   Connelly, J.N., Bollard, J., and Bizzarro, M. (2017) Pb-Pb chronometry and the early Solar System.

258   Geochimica et Cosmochimica Acta, 201, 345-363.

259   Daulton, T.L., Eisenhour, D.D., Bernatowicz, T.J., Lewis, R.S., and Buseck, P.R. (1996) Genesis of

260   presolar diamonds: comparative high-resolution transmission electron microscopy study of

261   meteoritic and terrestrial nano-diamonds. Geochimica et Cosmochimica Acta, 60, 4853-4872.

262   DeCarli, P.S., and Jamieson, J.C. (1961) Formation of diamond by explosive shock. Science, 133,

263   1821-1822.

264   El Goresy, A., Dera, P., Sharp, T., Prewitt, C. T., Chen, M., Dubrovinsky, L., Wopenka, B., Boctor, N.

265   Z., and Hemley, R. J. (2008) Seifertite, a dense orthorhombic polymorph of silica from the

266   Martian meteorites Shergotty and Zagami. European Journal of Mineralogy, 20, 523-528.

267   Erskine, D.J., and Nellis, W.J. (1991) Shock-induced martensitic phase-transformation of oriented

268   graphite to diamond. Nature, 349, 317-319.

269   Garvie, L.A.J., and Buseck, P.R. (2004) Nanosized carbon-rich grains in carbonaceous chondrite

270   meteorites. Earth and Planetary Science Letters, 224, 431-439.

271   Garvie, L.A.J. (2005) Extraterrestrial carbon nanospheres. Carbon, 44, 158–160.

272   Garvie, L.A.J. (2006) Surface electronic states of meteoritic nanodiamonds. Meteoritics and Planetary

273   Science, 41, 667-672.

274   Garvie L.A.J., and Buseck P.R. (2006) Carbonaceous materials in the acid residue from the Orgueil

275   carbonaceous chondrite meteorite, Meteoritics and Planetary Science, 41, 633-642.

276   Garvie, L.A.J., Németh, P., and Buseck, P.R. (2011) Diamond, bucky-diamond, graphite-diamond, Al-

277   silicate and stishovite in the Gujba CB chondrite. Meteoritics and Planetary Science, 46, A75.

278   Garvie, L.A.J., Németh, P., and Buseck P.R. (2014) Transformation of graphite to diamond via a

279   topotactic mechanism. American Mineralogist, 99(2-3), 531-538.

280   Garvie, L.A.J., Knauth, L. Paul., and Morris, M.A. (2017) Sedimentary laminations in the Isheyevo

281   (CH/CBb) carbonaceous chondrite formed by gentle impact-plume sweep-up. Icarus, 292, 36-47.

282   Huss, G.R., and Lewis, R.S. (1995) Presolar diamond, SiC, and graphite in primitive chondrites:

283   abundances as a function of meteorite class and petrologic type. Geochimica et Cosmochimica

284   Acta, 59, 115-160.

285   Kis, V.K., Shumilova, T., and Masaitis, V. (2016) HRTEM study of Popigai impact diamond:

286   heterogeneous diamond nanostructures in native amorphous carbon matrix. Physics and

287   Chemistry of Minerals, 43, 661-670.

288   Krot, A.N., Amelin, Y., Cassen, P., and Meibom, A. (2005) Young chondrules in CB chondrites from a

289   giant impact in the early Solar System. Nature, 436, 989–992.

290   Krot, A.N, Yurimoto, H, McKeegan, K., Leshin, L., Chaussidon, M., Libourel, G., Yoshitake, M.,

291   Huss, G., Guan, Y., and Zanda, B. (2006) Oxygen isotopic compositions of chondrules:

292   Implications for evolution of oxygen isotopic reservoirs in the inner solar nebula. Chemie der

293   Erde – Geochemistry, 66(4), 249-276.

294   Kuznetsov, V.L., Chuvilin, A.L., Butenko, Y.V., Mal'kov, I.Y., and Titov, V.M. (1994a) Onion-like

295   carbon from ultra-disperse diamond. Chemical Physics Letters, 222, 343–348.

296   Kuznetsov, V.L., Chuvilin, A.L., Moroz, E.M., Kolomiichuk, V.N., Shaikhudtdinov, S.K.,

297   Butenko, Y.V., and Mal'kov, I.Y. (1994b) Effect of explosion conditions on the structure of

298   detonation soots: Ultradisperse diamond and onion carbon. Carbon, 32, 873–882.

299   Le Guillou, C., Rouzaud, J. N., Remusat, L., Jambon, A., and Bourot-Denise, M. (2010) Structures,

300   origin and evolution of various carbon phases in the ureilite Northwest Africa 4742 compared

301   with laboratory-shocked graphite. Geochimica et Cosmochimica Acta, 74, 4167-4185.

302   Marty, B., Kelley, S., and Turner, G. (2010) Chronology and shock history of the Bencubbin meteorite:

303   a nitrogen, noble gas, and Ar-Ar investigation of silicates, metal and fluid inclusions. Geochimica

304   et Cosmochimica Acta, 74, 6636–665.

305   Morris, M.A., Garvie, L.A.J., and Knauth, L.P. (2015) New insight into the Solar System's transition

306   disk phase provided by the metal-rich carbonaceous chondrite Isheyevo. The Astrophysical

307   Journal Letters, 801, L22.

308   Murri, M., Smith, R.L., McColl, K., Hart, M., Alvaro, M., Jones, A.P., Németh, P., Salzmann, C.H.,

309   Corá, F., Domeneghetti, M.C., Nestola, F., Sobolev, N.V., Vishnevsky, S.A., Logvinova, A.M.,

310   and McMillan, P.F. (2019) Quantifying hexagonal stacking in diamond. Scientific Reports, 9,

311   10334.

312   Nakamura-Messenger, K., Messenger, S., Keller, L.P., Clemett, S.J., and Zolensky, M.E. (2006)

313   Organic globules in the Tagish Lake meteorite: remnants of the protosolar disk. Science, 314,

314   1439-1442.

315   Naraoka, H., Mita, H., Komiya, M., Yoneda, S., Kojima, H., and Shimoyama, A. (2004) A chemical

316   sequence of macromolecular organic matter in the CM chondrites. Meteoritics and Planetary

317   Science, 39, 401–406.

318   Németh, P., Garvie, L.A.J., Aoki, T., Dubrovinskaia, N., Dubrovinsky, L., and Buseck, P.R. (2014)

319   Lonsdaleite is faulted and twinned cubic diamond and does not exist as a discrete material. Nature

320   Communications, 5, 6447.

321   Németh, P., Garvie, L.A.J., and Buseck, P.R. (2015) Twinning of cubic diamond explains reported

322   nanodiamond polymorphs. Scientific Reports, 5, 18381.

323   Ohfuji, H., Irifune, T., Litasov, K.D., Yamashita, T., Isobe, F., Afanasiev, V.P., and Pokhilenk, N.P.

324   (2015) Natural occurrence of pure nano-polycrystalline diamond from impact crater. Scientific

325   Reports, 5, 14702.

326   Qin, L-C., and Iijima, S. (1996) Onion-like graphitic particles produced from diamond. Chemical

327   Physics Letters, 262(3-4), 252–258.

328 Pearson, V.K., Sephton, M.A., Franchi, I.A., Gibson, J.M., and Gilmour, I. (2006) Carbon and nitrogen

329   in carbonaceous chondrites: Elemental abundances and stable isotopic compositions. Meteoritics

330   and Planetary Science, 41, 1899-1918.

331 Sano, N., Wang, H., Chhowalla, M., Alexandrou, I., and Amaratunga, G.A.J. (2001) Synthesis of

332   carbon 'onions' in water. Nature, 414, 506.

333 Sharp, T.G., and DeCarli, P.S. (2006) Shock Effects in Meteorites. In D.S.M.J. Lauretta, H.Y., Ed.

334   Meteorites and the Early Solar System II, p. 653-678. The University of Arizona Press.

335 Sharp, T.G., Lingemann, C.M., Dupas, C., and Stöffler, D. (1997) Natural occurrence of $MgSiO_3$-

336   ilmenite and evidence for $MgSiO_3$-perovskite in a shocked L chondrite. Science, 277, 352–355.

337 Sharp, T.G., El Goresy, A., Wopenka, B., and Chen M. (1999) A post-stishovite SiO2 polymorph in the

338   meteorite Shergotty: implications for impact events. Science, 284, 1511-1513.

339 Shumilova, T., Kis, V.K., Masaitis, V., Sergey, I., and Boris M. (2014) Onion-like carbon in impact

340   diamonds from the Popigai astrobleme. European Journal of Mineralogy, 26, 267-277.

341 Smith, P.P., and Buseck, P.R. (1981) Graphitic carbon in the Allende meteorite: a microstructural

342   study. Science, 212, 322—324.

343 Stecher, T.P. (1965) Interstellar Extinction in the Ultraviolet. Astrophysical Journal, 142, 1683-1684.

344 Steele, A., McCubbin, F.M., Fries, M.D., Golden, D.C. Ming, D.W., and Benning L.G. (2012) Graphite

345   in the martian meteorite Allan Hills 84001. American Mineralogist, 97, 1256–1259.

346 Raty, J-Y., Galli, G., Bostedt, C., van Buuren, T.W., and Terminello, L.J. (2003) Quantum

347   Confinement and Fullerenelike Surface Reconstructions in Nanodiamonds. Physical Review

348   Letters 90, 037401.

349 Rubin, A.E., Kallemeyn, G.W., Wasson, J.T., Clayton, R.N., Mayeda, T.K., Grady, M.,

350   Verchovsky, A.B., Eugster, O., and Lorenzetti, S. (2003) Formation of metal and

351   silicate globules in Gujba: A new Bencubbin-like meteorite fall. Geochimica et

352   Cosmochimica Acta, 67, 3283–3298.

353 Terrones, H., and Terrones, M. (1997) The transformation of polyhedral particles into graphitic onions.

354   Journal of Physics and Chemistry of Solids, 58 (11), 1789-1796.

355 Ugarte, D. (1992) Curling and closure of graphitic networks under electron-beam irradiation. Nature,

356   359(6397), 707–709.

357 Weisberg, M.K., and Kimura, M. (2004) Petrology and Raman spectroscopy of shock phases in the

358   Gujba CB chondrite and the shock history of the CB parent body. Lunar and Planetary Science

359   Conference, XXXV, Abstract 1599.

360 Weisberg, M.K., Kimura, M., Suzuki, A., Ohtani, E., and Sugiura, N. (2006) Discovery of coesite and

361   significance of high pressure phases in the Gujba CB chondrite. Lunar and Planetary Science

362   Conference, XXXVII, Abstract 1788.

363 Weisberg, M.K., and Kimura, M. (2010) Petrology and Raman spectroscopy of high pressure phases in

364   the Gujba CB chondrite and the shock history of the CB parent body. Meteoritics and Planetary

365   Sciences, 45, 873–884.

366 Wright, E.L. (1988) The ultraviolet extinction from interstellar graphitic onions. Nature, 336, 227-228.

367 Xiao, J., Ouyang, G., Liu, P., Wang, C.X., and Yang, G.W. (2014) Reversible Nanodiamond-Carbon

368   Onion Phase Transformations. Nano Letters, 14, 3645−3652.

369 Yamada, K., and Tanabe, Y. (2002) Shock-induced phase transition of oriented pyrolytic graphite to

370   diamond at pressures up to 15 GPa. Carbon, 40, 261-269.

371   .

372

373

374

375

376

Figures

377

378 Figure 1. Un-shocked carbonaceous materials from the Gujba meteorite. **a**) A cluster of 2-3-nm-sized

379 nanodiamonds. White lines mark diamond {111} spacings (0.206-nm). **b)** Compact amorphous

380 carbonaceous nanosphere. **c)** Hollow carbonaceous nanosphere. Black arrows point to 0.34-nm

381 spacings indicative for graphitic material.

382

383 Figure 2. Representative HRTEM images of cage-like nanostructured carbonaceous materials. Black

384 arrows point to 0.34-nm spacings of graphite. **a**) A hollow 20-nm-sized nano-onion. **b**) A hollow 14-

385 nm-sized nano-onion. **c**) A deformed 20-nm-sized hollow nano-onion. **d**) A 7-nm-sized hollow nano-

386 onion. White arrow points to nanodiamond outside the nano-onion. Visible are the 0.21-nm spacings of

387 diamond {111}. **e)** An 8-nm-sized nano-onion with a core showing 0.21-nm spacings (white lines). The

388 onion is attached to an incompletely transformed graphite-diamond particle (white arrow). **f)** An 8-nm-

389 sized nano-onion with a core having 0.21-nm spacings (white lines).

390

391 Figure 3. HRTEM lattice-fringe image of a nano-onion containing graphite. **a)** A 10-nm-sized nano-

392 onion with graphite in its central part. Black arrows point to 0.34-nm spacings of graphite.

393 **b**) The FFT, calculated from the area marked by white corners of **a)**, shows hexagonally arranged

394 reflections with 0.21-nm spacings consistent with graphite projected along <001>. **c)** Background

395 filtered image, calculated from **a)** by selecting the reflections of **b)** enhances the visibility of graphite

396 cross-fringes. White arrows mark {100} planes of graphite with 0.212-nm spacings.

397

398 Figure 4. HRTEM lattice-fringe image of a 10-nm-sized bucky-diamond. The FFT (lower right corner)

399 shows {111} diamond reflections in <110> projections. White arrows mark {111} planes of diamond

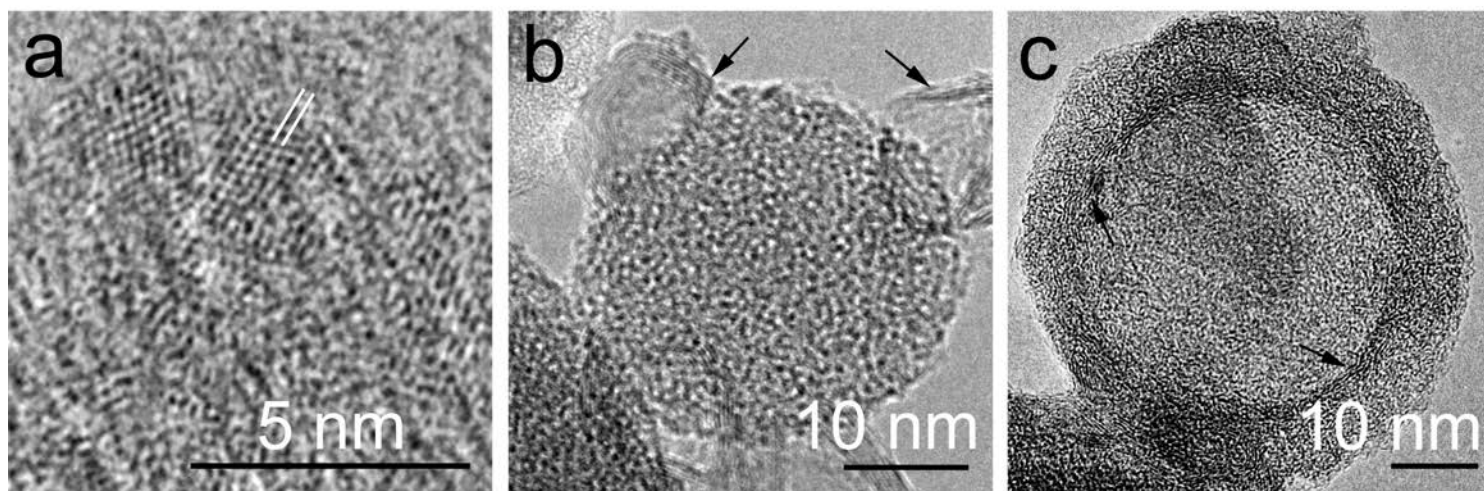400 with 0.206-nm spacings on the background filtered image (upper right corner).
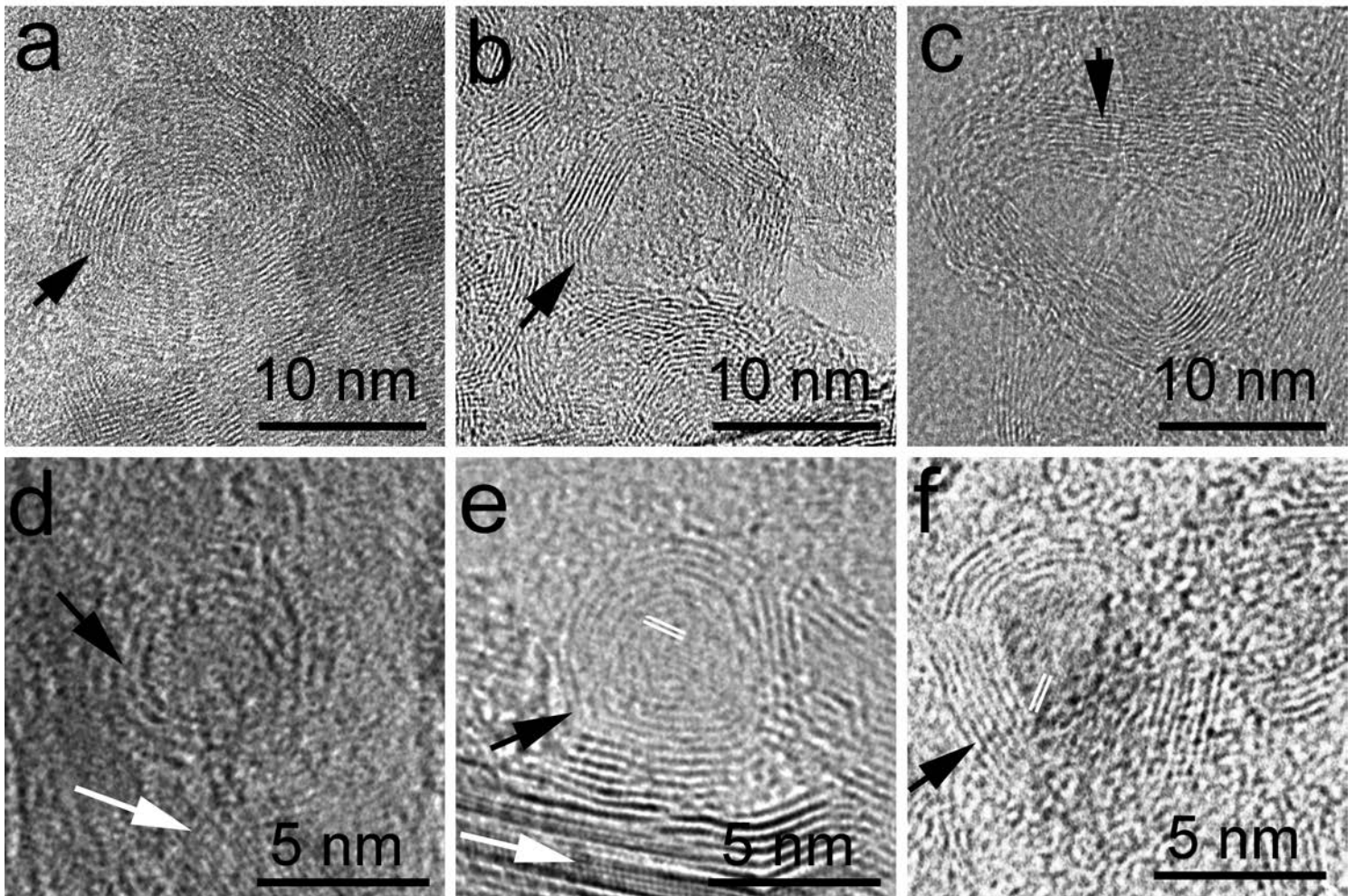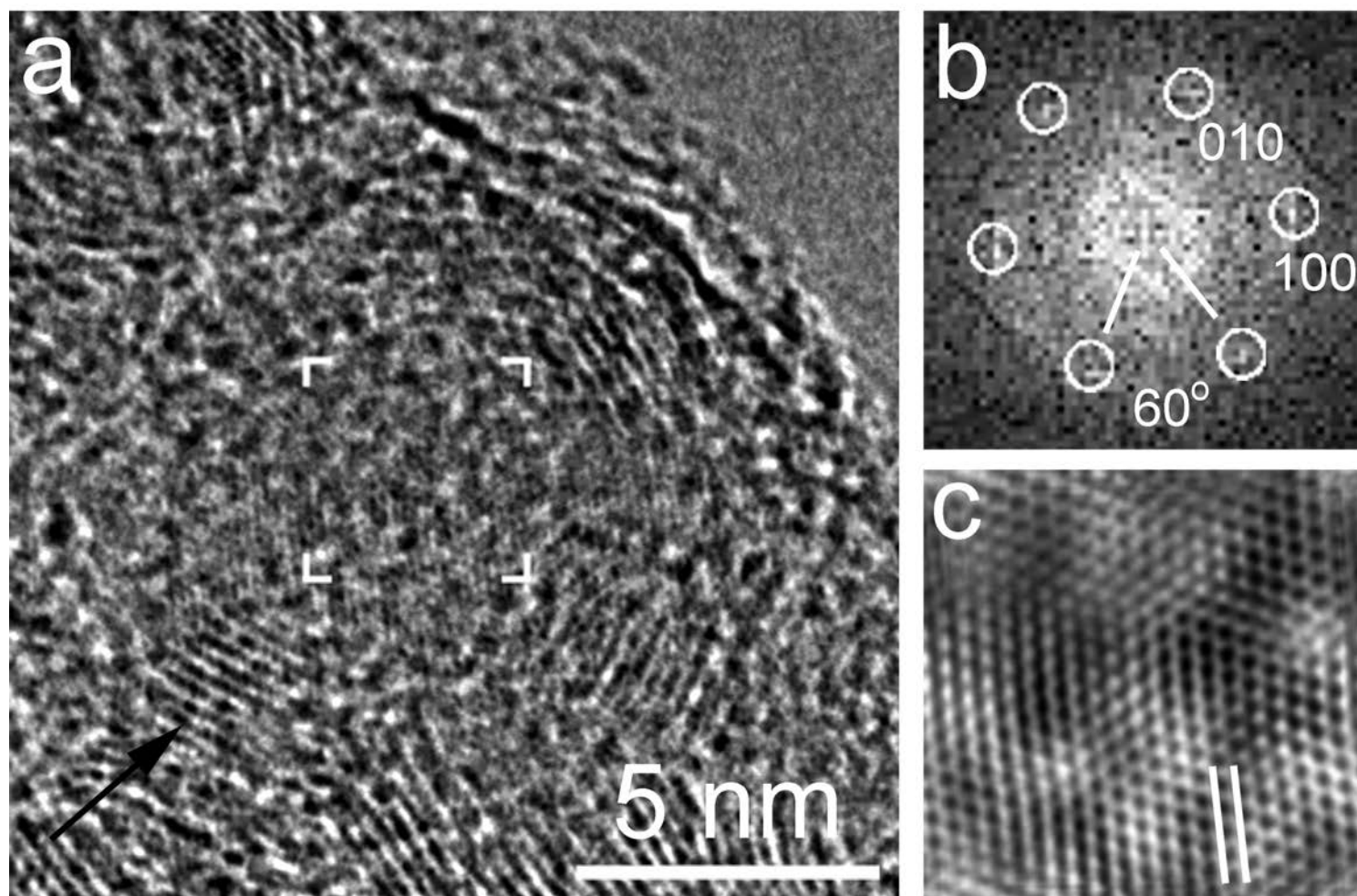
Fig. 1

Fig. 2

Fig. 3

Fig. 4